The RMT method for many-electron atomic systems in intense short-pulse laser light

L.R. Moore [a] , M.A. Lysaght [a] , L.A.A. Nikolopoulos [b] , J.S. Parker [a] , H.W. van der Hart [a] &
K.T. Taylor [a]

[a] Centre for Theoretical Atomic, Molecular and Optical Physics , School of Mathematics and
Physics, Queen's University Belfast , Belfast BT7 1NN, UK
[b] School of Physical Sciences , Dublin City University , Dublin 9, Ireland
Published online: 26 Feb 2011.

PLEASE SCROLL DOWN FOR ARTICLE

The RMT method for many-electron atomic systems in intense short-pulse laser light

L.R. Moore[a]*, M.A. Lysaght[a], L.A.A. Nikolopoulos[b],
J.S. Parker[a], H.W. van der Hart[a] and K.T. Taylor[a]

[a]*Centre for Theoretical Atomic, Molecular and Optical Physics, School of Mathematics and Physics, Queen's University Belfast, Belfast BT7 1NN, UK;* [b]*School of Physical Sciences, Dublin City University, Dublin 9, Ireland*

We describe a new *ab initio* method for solving the time-dependent Schrödinger equation for multi-electron atomic systems exposed to intense short-pulse laser light. We call the method the *R*-matrix with time-dependence (RMT) method. Our starting point is a finite-difference numerical integrator (HELIUM), which has proved successful at describing few-electron atoms and atomic ions in strong laser fields with high accuracy. By exploiting the *R*-matrix division-of-space concept, we bring together a numerical method most appropriate to the multi-electron finite inner region (*R*-matrix basis set) and a different numerical method most appropriate to the one-electron outer region (finite difference). In order to exploit massively parallel supercomputers efficiently, we time-propagate the wavefunction in both regions by employing Arnoldi methods, originally developed for HELIUM.

Keywords: multi-electron; *R*-matrix; finite-difference; strong laser fields; high performance computing

1. Introduction

Over the last several decades, increasing experimental interest in strongly time-dependent atomic and molecular systems [1–7] has been a driving force in the development of new computational and theoretical methods for calculating the dynamical response of atoms and molecules to intense laser radiation. In this paper we discuss recent extensions to computational methods [8–14] that enable application to complex atoms and molecules.

Advances in laser technology and in detection techniques [15,16] steadily increase the possibilities and refinement of experimental measurement. For instance, angular information regarding the emission of two electrons can now be gained and the Free Electron Lasers that have become operational are making available unprecedented high laser-light intensities in the ultraviolet to soft X-ray regimes [17,18]. Alongside advances in the short wavelength regime, the recent generation of light pulses with durations in the attosecond range (1 as $= 10^{-18}$ s) [19] heralds an exciting new era in ultrafast science. These pulses have opened up the possibility for the measurement and possible control of inner-shell electron dynamics inside atoms and molecules. A wide variety of attosecond experimental techniques have been demonstrated so far [20] which have led to the first real-time observations of

the decay of an inner-shell vacancy [21] and of interference effects in the double ionization of Ne due to shake-up processes [22]. If theory is to play a meaningful role, and especially a predictive one, in such circumstances, then sophisticated methods of calculation are required which will be capable of accurately describing both the multi-electron atomic structure and the multi-electron response to the light field.

We therefore take the opportunity in this article to detail how we have brought together various methods, developed in Belfast over the past 40 years, in an efficient and genuinely multi-electron treatment of a complex atom exposed to short-pulse laser light. Such a treatment must go after the time-dependent Schrödinger equation (TDSE) directly and thus a procedure which efficiently propagates an accurate solution of this equation forward in time (especially on massively-parallel supercomputers) is a first essential. To this end we first developed the Arnoldi method in its application to the TDSE some years ago [8]. Secondly, we found finite-difference (FD) methods invaluable in representing one- or two-electron wavefunctions over large radial distances and, moreover, combined FD methods with the Arnoldi propagator [8]. Thirdly, it is clear that in the ionisation of complex atoms almost all the electrons remain within around 20 Bohr radii of the nucleus. But within this 20 Bohr radii a multi-electron

representation is essential in order to allow for the various photon absorption and electron excitation and exchange processes that can occur there. We can handle this multi-electron representation via a close-coupling wavefunction form [23] and efficiently limit it to the appropriate region surrounding the nucleus by the use of the *R*-matrix method [24]. Indeed the separation of space by the *R*-matrix method allows further flexibility. Specifically it makes possible the use of the FD method for the one (or at most two) of the electrons located in the large-radial-extent outer region whilst still invoking a basis set form over the multi-electron inner region. This combination, taken together with the Arnoldi propagator [25] applied to both regions, brings us finally to the desired efficient and genuinely multi-electron treatment of a complex atom exposed to short-pulse laser light.

The paper is organised as follows. In Section 2 we present details of the new method we have developed for solving the TDSE for multi-electron atomic systems exposed to intense short-pulse laser light. We call the method the *R*-matrix with time-dependence (RMT) method. We describe the separation of position space into an outer and an inner region, and in Sections 2.1 and 2.2 we describe the direct integration of the TDSE in each of these regions, respectively. In Section 3 we report initial results pertaining to single-ionisation of helium and of neon at a laser wavelength of 248 nm. By comparing these ionisation rates with those obtained from other, independent, methods we confirm the accuracy of the new RMT method. We end the paper with some concluding remarks in Section 4.

2. The *R*-matrix with time-dependence (RMT) method

One *ab initio* approach capable of treating multi-electron systems is *R*-matrix theory, with the basic formulation appearing first in the context of nuclear theory, and later on applied in the field of atomic physics [23,26,27]. In the *R*-matrix method the position space occupied by the electrons is divided into two regions: an inner region (region I) surrounding the nucleus where a multi-electron wavefunction is constructed and multi-electron atom–laser Hamiltonian matrix elements are calculated explicitly, and an outer region (region II), chosen such that only one electron (or at most two) is present and the electron there, besides experiencing the laser field directly, is aware of the remainder of the atomic system only via long-range multi-pole interactions.

Traditionally, *R*-matrix theory is a theory where time is not explicitly involved in the study of the collision or photoionisation processes. However, for the description of complex multi-electron systems irradiated by short-pulse laser light a direct integration of the TDSE is required. To this end we have borrowed from the central concept of *R*-matrix theory, i.e. the reduction of the laser–atom problem into a 'complex' inner region close to the nucleus, in which electron–electron interactions are fully described and for which a method based on *R*-matrix eigenstates appears to be both accurate and tractable, and a 'simple' outer region, in which an effective one-electron (or possibly two-electron) problem is solved using the state-of-the-art grid-based technology. In both regions we integrate the TDSE directly.

Figure 1 displays the division of multi-electron position space which underlies *R*-matrix theory. In region I the time-dependent wavefunction is expanded over the *R*-matrix eigenstates of the field-free Hamiltonian. Region I is defined by all $N+1$ electrons of the system having a radial co-ordinate $r_q \leq b$, $q = 1, \ldots, N+1$. Region II is defined by N electrons having a radial coordinate $r_q \leq b$, $q = 1, \ldots, N$ and one electron having its radial coordinate $r_{N+1} > b$.
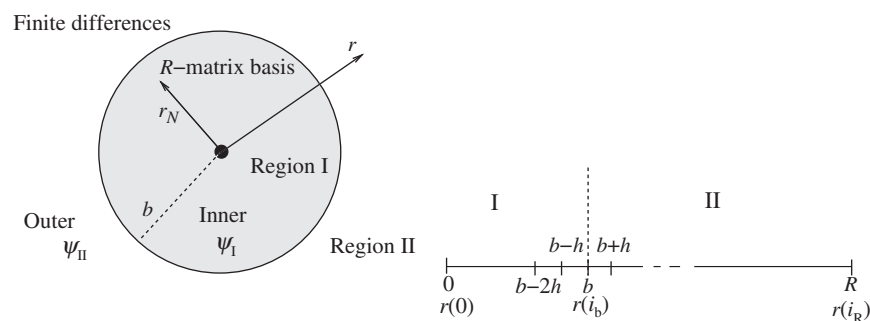
Figure 1. Partition of the configuration space for the electron coordinate. In the inner region I an eigenstate expansion representation of the wavefunction is chosen, while in the outer region II a grid representation is considered. The boundary of region I is at $r = b$ and the outer boundary of region II is at $r = R$. The radial variable of the $(N+1)$th electron is denoted as r. The grid points in region II are denoted by i, where i_b is the grid point on the boundary with region I and i_R is the grid point on the outer region boundary. The spacing between grid points is denoted by h.

In region II the time-dependent wavefunction is represented radially over a finite-difference grid by its values at equidistant grid points $r_{N+1}(i) = ih$, $i = i_b$, $i_b + 1, \ldots, i_R$. In both regions an explicitly time-dependent treatment of the laser–atom interaction is handled.

The basics of the method have recently been set out for the hydrogen atom [28]. A high-order Taylor propagator was employed there and the feasibility of combining basis set methods with finite-difference methods for describing the laser–atom interaction was firmly established. We have adapted the method to employ the Arnoldi propagator [25] throughout both spatial regions to provide an efficient method for multi-electron systems. In Sections 2.1 and 2.2 we describe our approach to solving the TDSE in the outer region (region II) and in the inner region (region I), respectively.

2.1. Outer region

Following R-matrix theory [24], the time-dependent $(N+1)$-electron wavefunction beyond a certain distance can be written as

$$\Psi(X_{N+1}, t) = \sum_p \overline{\Phi}_p(X_N; \hat{r}_{N+1}, \sigma_{N+1}) \frac{1}{r} f_p(r, t), \quad r \geq b, \tag{1}$$

where the radial variable of the $(N+1)$th electron is denoted as $r_{N+1} = r$. We have written $X_{N+1} \equiv X_N$, $x_{N+1} \equiv x_1, x_2, \ldots, x_{N+1}$ where $x_i \equiv r_i \sigma_i$ are the space and spin coordinates of the ith electron. The $\overline{\Phi}_p(X_N; \hat{r}_{N+1}, \sigma_{N+1})$ are channel functions formed by coupling the target states of the residual ionic system $\Phi_p(X_N)$ with angular and spin parts of the ejected electron wavefunction. The time dependence of the wavefunction is contained within the radial channel functions $f_p(r, t)$ describing the radial motion of the ejected electron (in the pth channel). The antisymmetrisation operator is absent from the wavefunction expansion because only the $(N+1)$th electron is present at large radial distances, thereby making it distinguishable from the remaining N electrons.

Because the number of electrons in the outer region (region II) is limited to just one, the TDSE in the outer region is, for each state of the residual-ion, reduced in dimensionality to at most three, thus simplifying the computational problem considerably. The TDSE in the outer region is given by Equation (11). By projecting the known target functions $\overline{\Phi}_p(X_N; \hat{r}_{N+1}, \sigma_{N+1})$ onto the TDSE and integrating over all spatial variables except the radial coordinate of the ejected electron, the following set of coupled partial differential equations for the radial channel functions $f_p(r, t)$ is obtained:

$$i \frac{\partial}{\partial t} f_p(r, t) = h_{II_p}(r) f_p(r, t) + \sum_{p'} \Big[W_{E_{pp'}}(r) + W_{D_{pp'}}(t) + W_{P_{pp'}}(r, t) \Big] f_{p'}(r, t), \tag{2}$$

where

$$h_{II_p}(r) = -\frac{1}{2} \frac{d^2}{dr^2} + \frac{l_p(l_p + 1)}{2r^2} - \frac{Z - N}{r} + E_p, \tag{3}$$

$$W_{E_{pp'}}(r) = \left\langle r^{-1} \overline{\Phi}_p \left| \sum_{j=1}^N \frac{1}{|\boldsymbol{r} - \boldsymbol{r}_j|} - \frac{N}{r} \right| r^{-1} \overline{\Phi}_{p'} \right\rangle, \tag{4}$$

$$W_{D_{pp'}}(t) = \left\langle r^{-1} \overline{\Phi}_p \left| \boldsymbol{E}(t) \cdot \sum_{i=1}^N \boldsymbol{r}_i \right| r^{-1} \overline{\Phi}_{p'} \right\rangle, \tag{5}$$

$$W_{P_{pp'}}(r, t) = \left\langle r^{-1} \overline{\Phi}_p \left| \boldsymbol{E}(t) \cdot \boldsymbol{r} \right| r^{-1} \overline{\Phi}_{p'} \right\rangle. \tag{6}$$

W_E, referred to as the long range potential in the R-matrix literature [24], is time-independent and arises from the electron–electron and electron–nuclear potential terms in the Hamiltonian. Time-dependence of these W_E terms could arise through the residual ion states entering the $\overline{\Phi}_p$ and $\overline{\Phi}_{p'}$ in Equation (4) individually carrying a time-dependence. However, the electron wavefunction which couples to these residual ion states is explicitly time-dependent and, via the present W_E, makes the linear combination of residual ion states a time-dependent quantity. W_D and W_P arise, respectively, from the interaction of the light field with the residual N-electron ion and from the interaction of the light field with the ejected electron and are defined in the above equations in the length gauge. E_p is the energy of the residual N-electron ion and l_p is the angular momentum of the outgoing electron.

To solve the set of coupled partial differential equations given in Equation (2) we employ finite difference methods. The radial channel functions $f_p(r,t)$ are discretised on an equidistant grid as depicted in Figure 1. The second derivative operator in Equation (2) is recast in a five-point finite difference representation. However, the inner boundary of the finite-difference region is not at the nucleus, where $r = 0$, but at some distance from the nucleus at $r = b$. The five-point finite-difference rule when applied to the radial channel function at the first grid point, $i = i_b$, thus requires information on the value of the radial channel function at points $i = i_b - 1$ and $i = i_b - 2$. (The function value at $i = i_b - 1$ is also needed when the rule is applied to the function at grid point $i = i_b + 1$.) These two grid points lie just inside the

outer boundary of the inner region. Since the wavefunction is assumed to be one-electron in nature moving outwards from the boundary at $r = b$, then, so long as b is chosen large enough, it can also be assumed that the wavefunction has still a one-electron character at the slightly smaller radial distance corresponding to the inner region grid point at $i = i_b - 2$ (this can also be enforced). In the inner region, the wavefunction is given by Equation (17) below. By projecting onto the target orbitals $\overline{\Phi}_p(X_N; \hat{r}_{N+1}, \sigma_{N+1})$ and integrating over all spatial variables except r (the radial coordinate of the ejected electron), the following radial wavefunction for the ejected electron in the inner region can be defined:

$$\bar{f}_p(r, t) = \sum_k C_k(t) f_{pk}(r), \quad 0 \le r \le b, \tag{7}$$

where $C_k(t)$ are the time-dependent coefficients in the basis expansion of the inner region wavefunction and $f_{pk}(r)$ represent inner region channel amplitudes. This equation is one of the main relations within our development because it links the time-dependent solutions of the inner and outer regions at the inter-region boundary (at $r = b$). By requiring $\bar{f}_p(b, t) = f_p(b, t)$ we obtain the following relation:

$$f_p(b, t) = \sum_k C_k(t) \omega_{pk}(b), \tag{8}$$

where $\omega_{pk}(b)$ are the known channel amplitudes evaluated on the boundary. They are defined explicitly by Equation (21) below. In an analogous fashion, we can obtain expressions for the radial wavefunctions at distances corresponding to the inner region grid points at $i = i_b - 1$ and $i = i_b - 2$ just inside the boundary at $r = b$:

$$f_p(b - h, t) = \sum_k C_k(t) \omega_{pk}(b - h), \tag{9}$$

$$f_p(b - 2h, t) = \sum_k C_k(t) \omega_{pk}(b - 2h). \tag{10}$$

Thus, knowing the basis expansion coefficients, $C_k(t)$ at time t means that the radial wavefunction of the ejected electron at inner-region points $i = i_b - 1$ and $i = i_b - 2$ can be obtained at time t. The finite-difference Hamiltonian may then be applied to the wavefunction in the outer region.

To propagate the outer region wavefunction forward in time, from time t to time $t + \delta t$, we employ the Arnoldi propagator [25]; its implementation is similar to that described in [8]. We assume that at time t the wavefunction is known throughout the inner and outer regions, a valid assumption since the ground state wavefunction will be known initially at $t = 0$. The first step is to form the radial wavefunctions of the ejected

electron in the inner region at $r = b - h$ and $r = b - 2h$ using Equations (9) and (10). This enables the outer region $H\Psi$ operation to be calculated. However, propagation involves computing not only $H\Psi$ but also $H^2\Psi$, $H^3\Psi, \ldots, H^n\Psi$ where n is the maximum propagation order. Therefore, at the points $i = i_b - 1$ and $i = i_b - 2$ it is not only the values of $f_p(r, t)$ which must be established, but also the values of $Hf_p(r, t)$, $H^2 f_p(r, t), \ldots, H^{n-1} f_p(r, t)$. One way in which these additional quantities may be calculated is by repeatedly applying the outer region Hamiltonian to $f_p(r, t)$ at the grid points $i = i_b - 1$ and $i = i_b - 2$. This ought to be permissible as the wavefunction at these two grid points should already consist only of the wavefunction of the one ejected electron. Once these quantities are calculated, the outer region wavefunction may be propagated forward one step in time using the Arnoldi propagator. We turn now to a discussion on the propagation of the inner region wavefunction.

2.2. Inner region

Neglecting relativistic effects, the behaviour of the inner region $N+1$ electron atomic system in the presence of the laser field is governed by the TDSE

$$i\frac{\partial}{\partial t} \Psi(X_{N+1}, t) = [H_{N+1} + D_{N+1}(t)]\Psi(X_{N+1}, t), \tag{11}$$

where the field-free Hamiltonian is

$$H_{N+1} = \sum_{i=1}^{N+1} \left(-\frac{1}{2}\nabla_i^2 - \frac{Z}{r_i} + \sum_{i>j=1}^{N+1} \frac{1}{r_{ij}} \right), \tag{12}$$

and where the dipole operator $D_{N+1}(t)$ is defined in the length gauge as

$$D_{N+1}(t) = E(t) \cdot \sum_{i=1}^{N+1} r_i. \tag{13}$$

We have taken the origin of the coordinates to be in the nucleus, which we assume has infinite mass. We have $r_{ij} = |r_i - r_j|$ where r_i and r_j are the vector coordinates of the ith and jth electrons. The use of the length gauge is in contrast to strong field calculations for one- and two-electron systems in which the velocity form of the dipole operator has been used with advantage. However, for the interaction of the laser field with a multi-electron atom near the nucleus, we have found, from previous investigations using basis set methods, that the laser field is in practice best described using the length form of the dipole operator [29,30].

However, in the inner region, the Hamiltonian H_{N+1} is not Hermitian owing to the presence of the kinetic energy $-\frac{1}{2}\nabla_i^2$ term in Equation (12) and the finite value of the wavefunction and its derivative

on the inner-region boundary. Consequently we introduce the Bloch operator

$$\mathcal{L}_{N+1} = \frac{1}{2}\sum_{i=1}^{N+1}\delta(r_i - b)\left(\frac{\mathrm{d}}{\mathrm{d}r_i} - \frac{g_0 - 1}{r_i}\right), \qquad (14)$$

which is such that $H_{N+1} + \mathcal{L}_{N+1}$ is Hermitian in the internal region for any value of the arbitrary constant g_0. We choose $g_0 = 0$. The TDSE in the internal region may then be written as

$$\mathrm{i}\frac{\partial}{\partial t}\Psi_1(X_{N+1}, t) = H_I(t)\Psi_1(X_{N+1}, t) - \mathcal{L}_{N+1}\Psi(X_{N+1}, t), \qquad (15)$$

where

$$H_\mathrm{I}(t) = H_{N+1} + \mathcal{L}_{N+1} + D_{N+1}(t) \qquad (16)$$

and where $\Psi_1(X_{N+1}, t)$ is the wavefunction defined over region I in Figure 1. Equation (15) is a key one to the method. The second term on the right-hand side compensates for the Bloch term introduced to make H_I Hermitian. Note that it makes a contribution only at $r = b$ and brings into play there $\Psi(X_{N+1}, t)$, a wavefunction form which we have defined throughout both regions. This term is central to any time propagation scheme in region I because it connects the wavefunction form $\Psi_1(X_{N+1}, t)$, which is multi-electron in nature, with a wavefunction form that, at $r = b$, represents a single electron and which, numerically, is obtained from region II.

In order to solve Equation (15) we expand the wavefunction $\Psi(X_{N+1}, t)$ in terms of eigenstates of the field-free Hamiltonian for each accessible total angular momentum, $L \leq L_{\max}$:

$$\Psi(X_{N+1}, t) = \sum_k C_k(t)\psi_k(X_{N+1}). \qquad (17)$$

The basis functions ψ_k have the form of a close-coupling expansion with pseudostates [24]. To set up the Hamiltonian matrix, $H(t)$ in Equation (15), we employ the R-matrix II suite of codes [31]. This set of codes provides eigenenergies for an atomic system within a box for a range of angular momenta and reduced dipole matrix elements between all the eigenstates. The code has recently been adapted by replacing the standard R-matrix continuum functions by a set of continuum functions based on B-splines [29].

By projecting Equation (15) onto the eigenstates $\psi_k(X_{N+1})$ we obtain the evolution equations for the time-dependent coefficients $C_k(t)$:

$$\mathrm{i}\frac{\mathrm{d}}{\mathrm{d}t}C_k(t) = \sum_{k'}H_{I_{kk'}}(t)C_{k'}(t) - \langle\psi_k|\mathcal{L}_{N+1}|\Psi\rangle. \qquad (18)$$

After some algebra we can rewrite the evolution equations for the time-dependent coefficients as

$$\frac{\mathrm{d}}{\mathrm{d}t}C_k(t) = -\mathrm{i}\sum_{k'}H_{I_{kk'}}(t)C_{k'}(t) + \frac{\mathrm{i}}{2}\sum_p\omega_{pk}\left.\frac{\partial f_p(r, t)}{\partial r}\right|_{r=b}, \qquad (19)$$

where

$$f_p(r, t) = \langle\overline{\Phi}_p r_{N+1}^{-1}|\Psi\rangle'_{r_{N+1}=r}, \qquad (20)$$

with the prime on the matrix elements denoting that the integral is carried out over space and spin coordinates of all $N + 1$ electrons except the radial coordinate r_{N+1} of the ejected electron. These reduced radial functions, $f_p(b, t)$ are analytical continuations of the functions defined in Section 2.1. The surface amplitudes, ω_{pk} have also been mentioned in Section 2.1 and are defined by

$$\omega_{pk} = \langle\overline{\Phi}_p r_{N+1}^{-1}|\psi_k\rangle'_{r_{N+1}=b}. \qquad (21)$$

Equation (19) represents an inhomogeneous differential equation due to the inclusion of the Bloch surface terms on the R-matrix boundary. In the rest of this subsection we present a numerical method for solving Equation (19) which enables the inner region wavefunction to be propagated forward one time-step from time t to time $t + \delta t$.

We rewrite Equation (19) in matrix notation as

$$\frac{\mathrm{d}}{\mathrm{d}t}\mathbf{C}(t) = -\mathrm{i}\mathbf{H}_\mathbf{I}(t)\mathbf{C}(t) + \mathrm{i}\mathbf{S}(t), \qquad (22)$$

where

$$S_k(t) = \frac{1}{2}\sum_p\omega_{pk}\left.\frac{\partial f_p(r, t)}{\partial r}\right|_{r=b}. \qquad (23)$$

The inhomogeneous TDSE of the form given in Equation (22) arises in many areas of quantum dynamics. In particular, it has been used in a time-dependent treatment of reactive scattering [32] and in optimal control theory using state dependent constraints [33]. To date, the inhomogeneous TDSE has been solved using split-propagator schemes [34] or via full diagonalisation of the Hamiltonian [33]. It has also recently been solved by employing a semi-implicit Crank–Nicholson method within an earlier time-dependent R-matrix framework [35]. However, it is only recently that attempts have been made at using high-order explicit methods to solve equations of the type given by Equation (22). Recently, a formal solution of the inhomogeneous TDSE has been derived which has been adapted to a Chebyshev propagation scheme [36]. An alternative simplified version of the high-order propagator for the inhomogeneous TDSE

can also be devised by approximating the formal solution explicitly by a Taylor expansion [36]. This is the method used for the single-electron implementation of the current method [28]. While the Taylor expansion approach has been shown to give accurate results for the case of hydrogen [28], using a Krylov subspace based approach, similar to that outlined in [8], would be more efficient especially when dealing with the large Hamiltonian matrices associated with complex multi-electron dynamics.

As shown in [36], the Taylor series for $\mathbf{C}(t + \delta t)$ in terms of $\mathbf{C}(t)$ is:

$$\mathbf{C}(t + \delta t) = \sum_{j=0}^{\infty} \delta t^j \sum_{k=0}^{\infty} \frac{(-\mathrm{i}\delta t \mathbf{H}_\mathrm{I})^k}{(k + j)!} \mathbf{U}_j(t), \quad (24)$$

where

$$\mathbf{U}_0(t) = \mathbf{C}(t), \quad \mathbf{U}_j(t) = \mathrm{i}\frac{\mathrm{d}^{j-1}}{\mathrm{d}t^{j-1}}\mathbf{S}(t). \quad (25)$$

Equation (24) can be rewritten in terms of so-called ϕ functions [37] as

$$\mathbf{C}(t + \delta t) = \exp(-\mathrm{i}\delta t \mathbf{H}_\mathrm{I})\mathbf{C}(t) + \sum_{j=1}^{\infty} \delta t^j \phi_j(-\mathrm{i}\delta t \mathbf{H}_\mathrm{I})\mathbf{U}_j(t). \quad (26)$$

The $\phi_j(-\mathrm{i}\delta t \mathbf{H}_\mathrm{I})$ functions are related to the exponentiation of the Hamiltonian matrix and are due to the time-dependent inhomogeneity in Equation (22). For a scalar argument z the $\phi_j(z)$ functions are defined by the integral representation

$$\phi_j(z) = \frac{1}{(j-1)!}\int_0^1 \exp[(1-\theta)z]\theta^{j-1}\,\mathrm{d}\theta, \quad j \geq 1. \quad (27)$$

for small values of j, these $\phi_j(z)$ functions are given by:

$$\phi_1(z) = \frac{\exp(z) - 1}{z},$$
$$\phi_2(z) = \frac{\exp(z) - 1 - z}{z^2},$$
$$\phi_3(z) = \frac{\exp(z) - 1 - z - \frac{1}{2}z^2}{z^3}. \quad (28)$$

The $\phi_j(z)$ functions satisfy the recurrence relation

$$\phi_{j+1}(z) = \frac{\phi_j(z) - (1/j!)}{z}, \quad \phi_0(z) = \exp(z), \quad j = 0, 1, 2, \ldots \quad (29)$$

and have the Taylor expansion

$$\phi_j(z) = \sum_{k=0}^{\infty} \frac{z^k}{(k+j)!}. \quad (30)$$

By suitably truncating the series in Equation (26), we obtain the approximation

$$\mathbf{C}(t + \delta t) \approx \hat{\mathbf{C}}(t + \delta t) = \exp(-\mathrm{i}\delta t \mathbf{H}_\mathrm{I})\mathbf{C}(t)$$
$$+ \sum_{j=1}^{n_j} \delta t^j \phi_j(-\mathrm{i}\delta t \mathbf{H}_\mathrm{I})\mathbf{U}_j(t). \quad (31)$$

The first term on the right-hand side of Equation (31) is the familiar solution to the homogeneous TDSE. In order to calculate this term we use an Arnoldi propagator; the procedure is similar to that outlined in [8]. For the calculation of the second term on the right-hand side of Equation (31) we also use a Krylov subspace based method to calculate the action of the $\phi_j(-\mathrm{i}\delta t \mathbf{H}_\mathrm{I})$ functions on the $\mathbf{U}_j(t)$ vectors passed from region II (see Figure 1). The method is similar to that used to calculate the action of $\exp(-\mathrm{i}\delta t \mathbf{H}_\mathrm{I})$ on $\mathbf{C}(t)$. We form a Krylov subspace for each of the vectors $\phi_j(-\mathrm{i}\delta t \mathbf{H}_\mathrm{I})\mathbf{U}_j$ entering the summation of Equation (31). We begin by approximating the vector $\phi_j(-\mathrm{i}\delta t \mathbf{H}_\mathrm{I})\mathbf{U}_j$ in a Krylov subspace $K_{n+1,j}$ spanned by the vectors $\mathbf{U}_j, \mathbf{H}_\mathrm{I}\mathbf{U}_j, \ldots, \mathbf{H}_\mathrm{I}^n\mathbf{U}_j$. Following the standard Arnoldi method we apply the Gram–Schmidt procedure to obtain an orthonormal set of vectors that span $K_{n+1,j}$ which we write as $\mathbf{Q}_{0,j}, \mathbf{Q}_{1,j}, \ldots, \mathbf{Q}_{n,j}$ where $\mathbf{Q}_{0,j} = \mathbf{U}_j/|\mathbf{U}_j|$. Let $\mathbf{Q}_j$ denote the matrix formed by the $n+1$ column vectors $(\mathbf{Q}_{0,j}, \mathbf{Q}_{1,j}, \ldots, \mathbf{Q}_{n,j})$. Then the n-by-n matrix $\mathbf{h}_j = \mathbf{Q}_j^\dagger \mathbf{H}_\mathrm{I}\mathbf{Q}_j$ is the projection of the action of $\mathbf{H}_\mathrm{I}$ on the Krylov subspace $K_{n+1,j}$ expressed in terms of the basis $\{\mathbf{Q}_{0,j}, \ldots \mathbf{Q}_{n,j}\}$.

We now approximate $\phi_j(-\mathrm{i}\delta t \mathbf{H}_\mathrm{I})\mathbf{U}_j$ by $\phi_j(-\mathrm{i}\delta t \mathbf{Q}_j\mathbf{h}_j\mathbf{Q}_j^\dagger)\mathbf{U}_j$. Since $\mathbf{Q}_j^\dagger \mathbf{Q}_j = \mathbf{I}$ and $\mathbf{Q}_j\mathbf{Q}_j^\dagger \mathbf{U}_j = \mathbf{U}_j$ we have $\phi_j(-\mathrm{i}\delta t \mathbf{Q}_j\mathbf{h}_j\mathbf{Q}_j^\dagger)\mathbf{U}_j = \mathbf{Q}_j\phi_j(-\mathrm{i}\delta t \mathbf{h}_j)\mathbf{Q}_j^\dagger \mathbf{U}_j$. The advantage of this formulation is that since the matrix $\mathbf{h}_j$ has size order n the evaluation of $\phi_j(-\mathrm{i}\delta t \mathbf{h}_j)$ is much cheaper than that of $\phi_j(-\mathrm{i}\delta t \mathbf{H}_\mathrm{I})$.

In recent years, there has been considerable effort made at developing efficient and accurate methods for computing the $\phi_j(z)$ functions. The most popular method for computing the matrix exponential (the $\phi_0(z)$ function) is the scaling and squaring method combined with the Padé approximation [38]. This method has recently been adapted to compute the closely related $\phi_j(z)$ functions with $j \geq 1$ [37]. The first method to take advantage of the Krylov subspace approach to calculate the action of $\phi_j(z)$ functions on a vector was developed several years ago [39]. In this method, the Arnoldi algorithm was extended in order to compute the $\phi_1(z)$ function that appears in the solution of linear ordinary differential equations with constant inhomogeneity. This work has very recently been generalised to compute the action of $\phi_j(z)$ functions on a vector with $j \geq 1$ [40]. In our current implementation the calculation of the $\phi_j(z)$ functions

is tackled by following an idea set out in [41] and generalized in [39] whereby the reduced matrix $\mathbf{h}_j$ is augmented to form a larger matrix given by

$$\hat{\mathbf{h}}_j = \begin{bmatrix} \mathbf{h}_j & \mathbf{e}_1 & 0 \\ 0 & 0 & \mathbf{I} \\ 0 & 0 & 0 \end{bmatrix}, \qquad (32)$$

where $\mathbf{e}_1$ is the first vector in the standard basis and the identity matrix, $\mathbf{I}$, has $j-1$ rows. Following the augmentation of $\mathbf{h}_j$, the top n entries of the last column of $\exp(-\mathrm{i}\delta t \hat{\mathbf{h}}_j)$ yield the vector $\phi_j(-\mathrm{i}\delta t\mathbf{h}_j)\mathbf{e}_1$. As an initial approach to computing the $\phi_j(z)$ functions we have followed this augmentation method and in the final step we compute $\exp(-\mathrm{i}\hat{\mathbf{h}}_j\delta t)$ using a degree-6 Padé approximant for general matrices, combined with scaling and squaring.

The procedure outlined above is repeated for each of the $\phi_j(-\mathrm{i}\delta t\mathbf{H}_\mathrm{I})\mathbf{U}_j$ terms in the summation on the right-hand side of Equation (31). Summing these n_j terms and adding to the first term on the right-hand side of Equation (31) then provides us with a means of propagating the wavefunction in the R-matrix inner region forward one step in time.

By this stage the wavefunction is known at time $t+\delta t$ throughout regions I and II and we can progress further in time by repeating, for successive time steps δt, the procedures described both in Section 2.1 above and in this section.

3. Results

As a means of demonstrating the accuracy of the new mixed R-matrix with time-dependence (RMT) method, we calculate single-electron ionisation rates for He and Ne irradiated by a laser pulse with a central wavelength of 248 nm corresponding to the fundamental wavelength of the KrF laser. We compare these rates with ionisation rates obtained using the time-independent R-matrix Floquet (RMF) method and, in the case of He, also with HELIUM [8].

For the RMT Ne calculations, we use in the inner-region the R-matrix basis developed for single-photon ionisation of Ne [27]. For the RMT He calculations we use the same basis as described in [42]. In both sets of calculations we use only the ground state of the residual ion as a target state and we truncate the eigenbasis by removing high lying eigenstates. The eigenbasis truncation has no adverse effect on the accuracy of our calculations. We typically use $L_{\max} = 11$–15 and an outer region finite difference mesh spacing (h in Figure 1) of 0.2 Bohr radii.

In order to obtain RMT ionisation rates that are comparable to the RMF results we irradiate He and Ne with pulses that typically consist of 20–30 cycles of

Table 1. Single-ionisation rates in atomic units obtained by RMT, by HELIUM and by the three-state approximation in the RMF approach for given values of the peak laser intensity.

Intensity ($10^{14}\,\mathrm{W\,cm^{-2}}$)	RMT	HELIUM	RMF
0.5	1.18×10^{-8}	1.25×10^{-8}	1.13×10^{-8}
1.78	2.77×10^{-7}		2.76×10^{-7}
3.2	1.27×10^{-5}	1.21×10^{-5}	1.23×10^{-5}
4.0	3.23×10^{-5}	3.15×10^{-5}	3.02×10^{-5}

the electric field, and therefore extend the outer region boundary to a radius of typically 500–1000 Bohr radii in order to prevent any reflections of the wavefunction. The ionisation rate is obtained by calculating the decrease in the norm of the inner region wavefunction beyond the R-matrix boundary distance, b, which we set to 20 Bohr radii for both He and Ne.

Table 1 shows a comparison of He single-electron ionisation rates for four intensities at 248 nm. Away from resonances, the ionisation rates calculated by RMT agree well (to within 10%) with those calculated by HELIUM [44] and by the RMF method [42]. At an intensity of $1.78 \times 10^{14}\,\mathrm{W\,cm^{-2}}$ there is a resonance with the 1s4p ^{1}P$^\mathrm{o}$ and 1s4f ^{1}F$^\mathrm{o}$ states. At this intensity the HELIUM ionisation rate is higher than the RMF rate by 22%. However, there is an uncertainty of $\pm 15\%$ in the rate calculated by HELIUM at this intensity. This is because the time-evolution of the decay of the inner region norm is complicated, exhibiting long-period oscillations and thus requiring integrations over greater than a hundred field periods. To avoid this complication and hence obtain a more precise ionisation rate with the RMT method, we measured the increase in population in the outer region beyond an extended radial distance of 250 Bohr radii, a distance from the origin which is more than sufficient to contain the resonant states. The resulting RMT ionisation rate is in very good agreement with the RMF rate.

Figure 2 shows the corresponding ionisation rates for Ne irradiated by a 248 nm laser pulse. The ionisation rates are compared to those obtained using the RMF method. Agreement between the two sets of results is very good, typically within 10% of each other away from resonance. We have also compared our results with those calculated using a separate time-dependent R-matrix method [35,44] and have found excellent agreement throughout. This alternative time-dependent R-matrix method also divides configuration space into an inner and outer region. However, instead of using a finite-difference method in the outer region it employs an R-matrix-propagator technique based on Green's functions. The method uses a
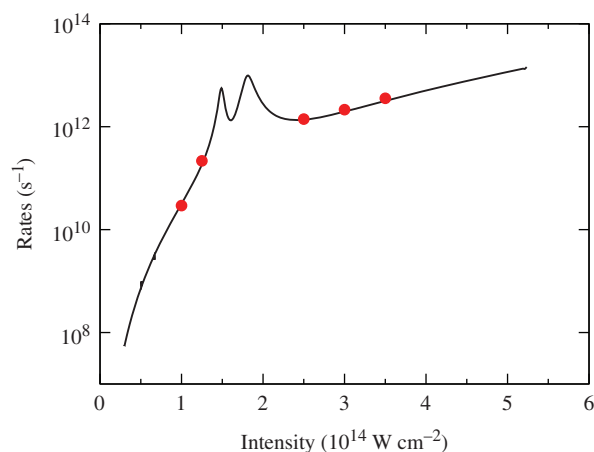
Figure 2. Comparison of ionisation rates for Ne irradiated by 248 nm laser light as a function of intensity. Rates from the current RMT approach (solid red circles) are compared to those obtained using the *R*-matrix Floquet approach (solid black line). (The colour version of this figure is included in the online version of the journal.)

Crank–Nicholson time propagator and has been successful at describing ultrafast correlated electron dynamics in multi-electron atoms [45].

4. Conclusion

We have detailed recent progress made in Belfast towards the goal of developing accurate theoretical methods for the description of atoms and molecules exposed to intense short laser pulses. Our recent work builds on well-established *ab initio* methods developed in Belfast over the last 40 years. One of the most successful of these methods has proven to be the full-dimensional finite-difference method and its associated computer code, HELIUM [8]. When combined with the Arnoldi propagator the finite-difference method allows for the highly accurate description of the response of few-electron atoms and molecules to short intense laser pulses.

We have described the extension of the underlying numerical methods of HELIUM in our development of a new *ab initio* time-dependent method for the description of multi-electron systems irradiated by intense short laser fields. We call the new method the *R*-matrix with time-dependence (RMT) method. The RMT method borrows from the powerful concept of *R*-matrix theory which divides the position space of the electrons surrounding the nucleus of the atom into a 'complex' inner region and a 'simple' outer region. In the outer region we use a grid representation of the wavefunction and propagation in space is obtained through the finite-difference method. We employ the Arnoldi propagator to propagate the wavefunction in

the time-domain. In the inner region *R*-matrix basis sets are used to describe the multi-electron wavefunction. Combining the inner region with the outer region requires the solution of an inhomogeneous TDSE in the inner region, which we have solved by extending significantly Arnoldi propagator techniques. We have demonstrated the accuracy of the new method by calculating ionisation rates for He and Ne irradiated by a 248 nm laser pulse. The ionisation rates obtained agree very well with those calculated using the time-independent *R*-matrix Floquet method and, in the case of He, also with those calculated using HELIUM.

While the current method has so far proved successful at describing the single-electron ionisation of multi-electron atoms, further development work is required. For example, we currently employ the length gauge in both spatial regions for the description of the laser–atom interaction. However, a transformation to a velocity gauge description in the outer-region is considered preferable due to the lower number of angular momenta required to obtain convergence in this gauge in this region. In the near future we intend to adapt the method so as to accurately describe the single-electron ionisation of a multi-electron molecule irradiated by intense short laser pulses. We also see the current method as forming a natural prerequisite for the development of a method that is capable of accurately describing the double-electron ionisation of atoms and molecules exposed to intense short laser pulses. Undoubtedly, such large-scale computations will involve design of computer codes that run efficiently on massively parallel supercomputers.

References

[1] Walker, B.; Sheehy, B.; DiMauro, L.F.; Agostini, P.; Schafer, K.J.; Kulander, K.C. *Phys. Rev. Lett*. **1994,** *73,* 1227–1230.
[2] Weber, T.H.; Giessen, H.; Weckenbrock, M.; Urbasch, G.; Staudte, A.; Spielberger, L.; Jagutzki, O.; Mergel, V.; Vollmer, M.; Dörner, R. *Nature* **2000,** *405,* 658–661.
[3] Lafon, R.; Chaloupka, J.L.; Sheehy, B.; Paul, P.M.; Agostini, P.; Kulander, K.C.; DiMauro, L.F. *Phys. Rev. Lett*. **2001,** *86,* 2762–2765.

[4] Staudte, A.; Ruiz, C.; Schöffler, M.; Schössler, S.; Zeidler, D.; Weber, Th.; Meckel, M.; Villeneuve, D.M.; Corkum, P.B.; Becker, A.; Dörner, R. *Phys. Rev. Lett.* **2007,** *99,* 263002.

[5] Rudenko, A.; de Jesus, V.L.B.; Ergler, Th.; Zrost, K.; Feuerstein, B.; Schröter, C.D.; Moshammer, R.; Ullrich, J. *Phys. Rev. Lett.* **2007,** *99,* 263003.

[6] Kreidi, K.; Akoury, D.; Jahnke, T.; Weber, Th.; Staudte, A.; Schöffler, M.; Neumann, N.; Titze, J.; Schmidt, L.Ph.H.; Czasch, A.; Jagutzki, O.; Costa Fraga, R.A.; Grisenti, R.E.; Smolarski, M.; Ranitovic, P.; Cocke, C.L.; Osipov, T.; Adaniya, V.; Thompson, J.C.; Prior, M.H.; Belkacem, A.; Landers, A.L.; Schmidt-Böcking, H.; Dörner, R. *Phys. Rev. Lett.* **2008,** *100,* 133005.

[7] Kelkensberg, F.; Lefebvre, C.; Siul, W.; Ghafur, O.; Nguyen-Dang, T.T.; Atabek, O.; Keller, A.; Serov, V.; Johnsson, P.; Swoboda, M.; Remetter, T.; L'Huillier, A.; Zherebtsov, S.; Sansone, G.; Benedetti, E.; Ferrari, F.; Nisoli, M.; Lépine, F.; Kling, M.F.; Vrakking, M.J.J. *Phys. Rev. Lett.* **2009,** *103,* 123005.

[8] Smyth, E.S.; Parker, J.S.; Taylor, K.T. *Comput. Phys. Commun.* **1998,** *114,* 1–14.

[9] Parker, J.S.; Moore, L.R.; Smyth, E.S.; Taylor, K.T. *J. Phys. B: At. Mol. Opt. Phys.* **2000,** *33,* 1057–1067.

[10] Dundas, D.; McCann, J.F.; Parker, J.S.; Taylor, K.T. *J. Phys. B: At. Mol. Opt. Phys.* **2000,** *33,* 3261–3276.

[11] Dundas, D. *Phys. Rev. A* **2002,** *65,* 023408.

[12] Parker, J.S.; Doherty, B.J.S.; Taylor, K.T.; Schultz, K.D.; Blaga, C.I.; DiMauro, L.F. *Phys. Rev. Lett.* **2006,** *96,* 133001.

[13] Moore, L.R.; Parker, J.S.; Meharg, K.J.; Armstrong, G.S.J.; Taylor, K.T. *J. Mod. Opt.* **2008,** *55,* 2541–2555.

[14] Parker, J.S.; Armstrong, G.S.J.; Boca, M.; Taylor, K.T. *J. Phys. B: At. Mol. Opt. Phys.* **2009,** *42,* 134011.

[15] Feuerstein, B.; Moshammer, R.; Fischer, D.; Dorn, A.; Schroter, C.D.; Deipenwisch, J.; Lopez-Urrutia, J.R.C.; Hohr, C.; Neumayer, P.; Ullrich, J.; Rottke, H.; Trump, C.; Wittmann, M.; Korn, G.; Sandner, W. *Phys. Rev. Lett.* **2001,** *87,* 043003.

[16] Kling, M.F.; Rauschenberger, J.; Verhoef, A.J.; Hasović, E.; Uphues, T.; Milošević, D.B.; Muller, H.G.; Vrakking, M.J.J. *New. J. Phys.* **2008,** *10,* 025024.

[17] Nagler, B.; Zastrau, U.; Fäustlin, R.R.; Vinko, S.M.; Whitcher, T.; Nelson, A.J.; Sobierajski, R.; Krzywinski, J.; Chalupsky, J.; Abreu, E.; Bajt, S.; Bornath, T.; Burian, T.; Chapman, H.; Cihelka, J.; Döppner, T.; Düsterer, S.; Dzelzainis, T.; Fajardo, M.; Förster, E.; Fortmann, C.; Galtier, E.; Glenzer, S.H.; Göde, S.; Gregori, G.; Hajkova, V.; Heimann, P.; Juha, L.; Jurek, M.; Khattak, F.Y.; Khorsand, A.R.; Klinger, D.; Kozlova, M.; Laarmann, T.; Lee, H.J.; Lee, R.W.; Meiwes-Broer, K.-H.; Mercere, P.; Murphy, W.J.; Przystawik, A.; Redmer, R.; Reinholz, H.; Riley, D.; Röpke, G.; Rosmej, F.; Saksl, K.; Schott, R.; Thiele, R.; Tiggesbäumker, J.; Toleikis, S.; Tschentscher, T.; Uschmann, I.; Vollmer, H.J.; Wark, J.S. *Nat. Phys.* **2009,** *5,* 693–696.

[18] Meyer, M.; Cubaynes, D.; Richardson, V.; Costello, J.T.; Radcliffe, P.; Li, W.B.; Düsterer, S.; Fritzsche, S.; Mihelic, A.; Papamihail, K.G.; Lambropoulos, P. *Phys. Rev. Lett.* **2010,** *104,* 213001.

[19] Sansone, G.; Benedetti, E.; Calegari, F.; Vozzi, C.; Avaldi, L.; Flammini, R.; Poletto, L.; Villoresi, P.; Altucci, C.; Velotta, R.; Stagira, S.; De Silvestri, S.; Nisoli, M. *Science* **2006,** *314,* 443–446.

[20] Krausz, F.; Ivanov, M. *Rev. Mod. Phys.* **2009,** *81,* 163–243.

[21] Drescher, M.; Hentschel, M.; Kienberger, R.; Uiberacker, M.; Yakovlev, V.; Scrinzi, A.; Westerwalbesloh, Th.; Kleineberg, U.; Heinzmann, U.; Krausz, F. *Nature* **2002,** *419,* 803–807.

[22] Uiberacker, M.; Uphues, Th.; Schultze, M.; Verhoef, A.J.; Yakovlev, V.; Kling, M.F.; Rauschenberger, J.; Kabachnik, N.M.; Schroder, H.; Lezius, M.; Kompa, K.L.; Muller, H.-G.; Vrakking, M.J.J.; Hendel, S.; Kleineberg, U.; Heinzmann, U.; Drescher, M.; Krausz, F. *Nature* **2007,** *446,* 627–632.

[23] Burke, P.G.; Seaton, M.J. *Methods Comput. Phys.* **1971,** *10,* 1–80.

[24] Burke, P.G.; Berrington, K.A. *Atomic and Molecular Processes: An R-matrix Approach*; IOP Publishing: Bristol, 1993.

[25] Arnoldi, W.E. *Quart. Appl. Math.* **1951,** *9,* 17–29.

[26] Burke, P.G.; Robb, W.D. *Adv. At. Mol. Phys.* **1976,** *11,* 143–214.

[27] Burke, P.G.; Taylor, K.T. *J. Phys. B: At. Mol. Opt. Phys.* **1975,** *8,* 2620–2639.

[28] Nikolopoulos, L.A.A.; Parker, J.S.; Taylor, K.T. *Phys. Rev. A* **2008,** *78,* 063420.

[29] van der Hart, H.W.; Lysaght, M.A.; Burke, P.G. *Phys. Rev. A* **2007,** *76,* 043405.

[30] Hutchinson, S.; Lysaght, M.A.; van der Hart, H.W. *J. Phys. B: At. Mol. Opt. Phys.* **2010,** *43,* 095603.

[31] Burke, P.G.; Burke, V.M.; Dunseath, K. *J. Phys. B: At. Mol. Opt. Phys.* **1994,** *27,* 5341–5373.

[32] Neuhauser, D. *Chem. Phys. Lett.* **1992,** *200,* 173–178.

[33] Paulo, J.P.; Kosloff, R.; Koch, C.P. *Phys. Rev. A* **2008,** *77,* 063412.

[34] Serban, I.; Werschnik, J.; Gross, E.K.U. *Phys. Rev. A* **2005,** *71,* 053810.

[35] Lysaght, M.A.; van der Hart, H.W.; Burke, P.G. *Phys. Rev. A* **2009,** *79,* 053411.

[36] Ndong, M.; Tal-Ezer, H.; Kosloff, R.; Koch, C.P. *J. Chem. Phys.* **2009,** *130,* 124108.

[37] Skaflestad, B.; Wright, W.M. *Appl. Numer. Math.* **2009,** *59,* 783–799.

[38] Moler, C.B.; Van Loan, C.F. *SIAM Rev.* **2003,** *45,* 3–49.

[39] Sidje, R. *ACM Trans. Math. Soft.* **1998,** *24,* 130–156.

[40] Niesen, J.; Wright, W.M. Technical Report. 2009, arXiv:0907.4631 e-Print archive. http://arxiv.org/abs/0907.4631 (accessed Feb 21, 2011).

[41] Saad, Y. *SIAM J. Numer. Anal.* **1992,** *29,* 209–228.

[42] Glass, D.H.; Burke, P.G. *J. Phys. B: At. Mol. Opt. Phys.* **2000,** *33,* 407–419.

[43] Parker, J.S.; Glass, D.H.; Moore, L.R.; Smyth, E.S.; Taylor, K.T.; Burke, P.G. *J. Phys. B: At. Mol. Opt. Phys.* **2000,** *33,* L239–L247.

[44] Lysaght, M.A.; Burke, P.G.; van der Hart, H.W. *Phys. Rev. Lett.* **2008,** *101,* 253001.

[45] Lysaght, M.A.; Burke, P.G.; van der Hart, H.W. *Phys. Rev. Lett.* **2009,** *102,* 193001.